



Islamic Republic of Iran  
Ministry of Science, Research and Technology



**Flemish Institute for Technological Research**  
Environmental Modeling Unit  
Boeretang 200, 2400 Mol, Belgium



**Faculty of Bioscience Engineering**  
Department of soil management  
Coupure Links 653 Bl. A, 9000 Gent

# Data assimilation of in situ soil moisture measurements in hydrological models

---

- Second annual doctoral progress report, work plan and achievements -

Applicant: Meisam Rezaei

Supervisor: - Prof. Dr. Ir. Piet Seuntjens,  
(VITO, Environmental Modeling Unit, and UGent,  
Department of Soil Management)

Co-Supervisors: - Dr. Ir. Ingeborg Joris  
(VITO, Environmental Modeling Unit)  
- Prof. Dr. Ir. Wim Cornelis  
(UGent, Department of Soil Management)

Date: May 2014

## Table of Contents

Management summary	4
Chapter 1 Introduction	6
1.1 <i>Scientific background</i>	6
1.2 <i>Aim of the research and research strategy</i>	7
1.3 <i>Summary of the research of the past year</i>	7
Chapter 2 Report of the past period	10
2.1 <i>Achieved Results</i>	10
2.1.1 <i>Further characterisation of study site 1 and soil</i>	10
2.1.2: <i>Soil hydrological model for a 2-layered sandy soil for irrigation management</i>	11
2.1.2.1 <i>Effect of the Bottom Boundary Condition and Parameter Uncertainty on Model Prediction</i>	11
2.1.2.2: <i>Model Calibration</i>	12
2.1.2.3: <i>Model Evaluation</i>	13
2.1.2.4: <i>Effect of Optimization Scenarios on Estimated Water Stress</i>	15
2.1.2.5: <i>Conclusion of the 1D soil hydrological modeling</i>	15
2.1.3: <i>Upscaling soil saturated hydraulic conductivity using ECa</i>	16
2.1.3.1: <i>Relation between soil hydraulic properties and ECa</i>	16
2.1.3.2: <i>Approach 1: Regression estimation of hydraulic properties from ECa measurements</i>	17
2.1.3.3: <i>Approach 2: Unsaturated hydraulic conductivity estimates from ECa</i>	17
2.2: <i>Scientific in- and output</i>	19
Chapter 3: Future perspectives	20
3.1 <i>Evaluation of the results and currently missing elements</i>	20
3.2 <i>Planning</i>	21
References	23

## List of abbreviations

$\theta_s$	saturated water content
$\theta_r$	residual water content
Ce	Nash–Sutcliffe coefficient of model efficiency
CTRS	central total sensitivity analysis
CV	coefficient of variation
DOE	depths of explorations
ECa	apparent soil electrical conductivity
ECw	soil water (fully saturated soil or soil solution)
EMI	electromagnetic induction
ET	evapotranspiration
ETo	reference evapotranspiration
FF	formation factor
GWL	ground water level
K(h)	unsaturated hydraulic conductivity
Ks	saturated hydraulic conductivity
MVG	van Genuchten-Mualem
OC	organic carbon
PTF	pedotransfer functions
$R^2$	coefficient of determination R –square
RMSE	root-mean-square deviation
Se	degree of saturation
SA	sensitivity analysis
$\theta(h)$	soil water retention curve
$\rho_b$	bulk density

## Management summary

Efficient water utilization and optimal water supply/distribution to increase food and fodder productivity are of utmost importance in confronting worldwide water scarcity, climate change, growing populations and increasing water demands. In this respect, irrigation efficiency, which is influenced by the type of irrigation and irrigation scheduling, is an essential issue for achieving higher productivity. To improve irrigation strategies in precision agriculture, soil water status can be more accurately described using a combination of advanced monitoring and modeling. Our study focuses on the combination of high resolution hydrological data with hydrological models that predict water flow and solute (pollutants and salts) transport and water redistribution in agricultural soils under irrigation. Field plots of a potato farmer in a sandy region in Belgium were instrumented to continuously monitor soil moisture and water potential before, during and after irrigation in dry summer periods. The aim is to optimize the irrigation process by combining online sensor field data with process based models. This research is part of Activity 305 'Precision agriculture and remote sensing' of the VITO GWO and is also part of the strategic cooperation with UGent within the platform 'Managing Natural Resources'.

Over the past 2 years, we applied a combination of in-situ monitoring and numerical modeling -Hydrus 1D- to estimate water content fluctuations in a heterogeneous sandy grassland soil under irrigation with water table fluctuating between 80 and 155 cm. Over the last year, more sampling and analyses were carried out to further characterize the hydraulic properties over the entire field. Modeling results for the field demonstrated clearly the profound effect of the position of the GWL, and to a lesser extent, the effect of spatially variable soil hydraulic properties ( $K_s$ ,  $n$  and  $\alpha$ ) on the estimated water content in the sandy two-layered soil under grass. Our results show that currently applied uniform water distribution using sprinkler irrigation seems not to be efficient since at locations with shallow groundwater, the amount of water applied will be excessive as compared to the plant requirements while in locations with a deeper GWL, requirements will not be met.

To derive the optimal parameter set best describing the measured soil moisture content, 37 optimization scenarios were conducted with two to six parameters using various parameter combinations for the two soil layers. The best performing parameter optimization scenario was a 2-parameter scenario with  $K_s$  optimized for each layer. The results showed a better identifiability of the parameters (less correlations among parameters) with equal performance as compared to three, four or six parameter optimization. Model predictions using the calibrated model (with data from 2012) for an independent data set of soil moisture data in the validation period (2013) showed satisfactory performance of the model in view of irrigation management purposes. Comparing the degree of water stress for different optimization scenarios of groundwater depth, showed that grass was exposed to water stress in summer in 2013 but not for such a long period as compared to the 2012 growing season. The degree of water stress simulated with Hydrus 1D suggested to increase the irrigation amount in 2012 and 2013 and at least one or two times in the summer (June and July) and further distributing the amount of irrigation during the growing season, instead of using a huge amount of irrigation later in the season, as is common practice by the farmer.

A second part of the study focused on finding a relation between measured soil hydraulic properties and apparent electrical conductivity EC<sub>a</sub>. Our measurements of hydraulic

properties of the field clearly confirm that there is considerable spatial variability in the field and that this has an impact on the simulation of soil moisture content. Therefore this should be taken into account when upscaling soil hydraulic properties to the field scale in order to understand and model flow, solute and energy fluxes in the field and develop strategies for efficient irrigation. Upscaling soil hydraulic properties to the field scale can be done by linking them to apparent electrical conductivity (ECa), which can be measured efficiently and inexpensively so a spatially dense dataset for describing within-field spatial soil variability can be generated. In this study relations between the spatial variation of soil hydraulic properties and apparent soil electrical conductivity ECa measured with EM38 and DUALEM-21S sensors at two depths of explorations (DOE) 0-50 and 0-100 cm were investigated. Two predictive modelling approaches, i.e. i) a simple regression and ii) applying Archie's laws for saturated and unsaturated conditions in combination with MVG equations, were developed and it was compared how they were able to explain the observed values of hydraulic parameters.

Results demonstrated the spatial variability and heterogeneity of ECa and soil hydraulic properties  $K_s$ ,  $\alpha$  and  $n$ . We derived a regression relationship between  $\log K_s$  and ECa measured with DUALEM ( $r^2 \geq 0.70$ ) and with EM38 ( $r^2 > 0.46$ ) sensors. The predicted results were tested vs measured data and confirmed that the performance of DUALEM<sub>p,100</sub>- $K_s$  model is relatively better than that of the same sensor with lower DOE and of the EM38 sensor (RMSE =  $1.31 \text{ cm h}^{-1}$ ,  $R^2 = 0.55$ ). The relationships between MVG shape parameters and ECa datasets were generally poor ( $0.05 < R^2 < 0.26$ ). In the second approach, we showed that the water retention curve can be translated to ECa- $(h)$  and ECa- $S_e$  relations by combining the MVG equations and Archie's law. Results also show that reformulating the MVG equations based on ECa- $S_e$  relationships can help to estimate unsaturated hydraulic conductivity at the field scale.

In the third year, a second study site has been set up in a nearby field where potatoes are grown and has been instrumented with soil moisture sensors, tensiometers, groundwater level loggers and a weather station. Field hydraulic properties for the field will be derived using the equations developed for the first study site and the modeling approach developed for the first field will be tested here. Also quasi 3D-modelling of water flow at the field scale will be conducted. In this modeling set-up, the field will be modeled as a collection of 1D-columns representing the different field conditions (combination of soil properties, GWL, root zone depth). Combining this model with crop based models such as LINGRA-N or Aquacrop gives a direct simulation of the impact of irrigation strategies on crop yield at the field scale.

**Keywords:** soil, Hydrus, modeling, water flow and solute transport, tensiometers, water content profile probes, sensitivity analysis,  $K_s$ , ECa, upscaling, model calibration, validation and optimization

## Chapter 1 Introduction

### 1.1 Scientific background

Precision irrigation needs new methods of accurate irrigation scheduling (Jones, 2004). Recently various irrigation scheduling approaches such as soil-based, weather-based, crop-based, and canopy temperature-based by e.g. remote sensing have been presented in literature (Evelt, et al., 2008, Jones, 2004, Mohanty, et al., 2013, Nasetto, et al., 2012, Pardossi, et al., 2009). Numerical models such as Hydrus contain numerical solutions of the Richards' equation (Richards, 1931) for water flow and root water uptake (Fernández-Gálvez, et al., 2006, Skaggs, et al., 2006, Vrugt, et al., 2001), which have recently gained popularity. To optimize water use efficiency using hydrological models, researchers require the determination of hydraulic properties (Šimůnek and Hopmans, 2002), conditions related to climatology (evapotranspiration and precipitation) at the upper boundary (Brutsaert, 2005, Li, et al., 2012, Nasetto, et al., 2012) and groundwater dynamics at the lower boundary of the soil profile (Gandolfi, et al., 2006). The Hydrus model has been used in a wide range of applications in irrigation management, for example, by Sadeghi and Jones (2012), Tafteh and Sepaskhah (2012), Akhtar, et al. (2013), and Satchithanantham, et al. (2014), water harvesting e.g. by Verbist, et al. (2012), and also to simulate the fate of nutrients and contaminants in soils e.g. Seuntjens, et al. (2001), Jiang, et al. (2010), Seuntjens (2002), Ebrahimian, et al. (2012), Cannavo, et al. (2013). The calibration process is crucial to identify sensitive parameters in a hydrological model for application to an entire field. To that end, systematical SA has been used to better estimate values, to better understand and reduce uncertainty (Rocha, et al., 2006) and to investigate the effects of various parameters or processes on water flow and transport (van Genuchten, et al., 2012). To reduce the number of parameters that need to be optimized, local SA are often performed that evaluate model output for each parameter perturbation in a one-at-a-time approach. Due to the highly parameterized framework of numerical hydrological models, direct measurement of its parameters may be inaccurate, insufficient or inefficient for predictions at the field scale (Verbist, et al., 2012, Wöhling, et al., 2008). This can be overcome by conducting inverse modeling. An example is the Levenberg–Marquardt optimization for single-objective inverse parameter estimation (Abbasi, et al., 2004, Abbasi, et al., 2003, Jacques, et al., 2012, Šimůnek, et al., 2013). Inverse simulation with Richards' equation-based models is generally carried out to obtain parameters of the van Genuchten (1980) water retention  $\theta(h)$  and hydraulic conductivity  $K(h)$  functions. Overview examples of the inverse modeling procedure can be found in Vrugt, et al. (2008) and Wöhling and Vrugt (2011).

Characterizing field scale hydraulic properties to predict and understand flow, solute and energy fluxes at the field is crucial for sustainable management and precision agriculture (Vereecken, et al., 2007) and accurate digital soil properties mapping (Chaplot, et al., 2011, Sudduth, et al., 2013). To practice site-specific management (e.g. precision irrigation) requires accurate information on spatial variation of the fields hydraulic properties and detailed observations (Carroll and Oliver, 2005). On the other hand, direct measurements of hydraulic properties (in the field or at the laboratory) not only are time consuming, labor intensive and expensive, but also perturb the system. Moreover, to have spatially representative observations, a high sampling density (in size and space) is required (Jury and Horton, 2004). Finding a link between hydraulic properties and other available ancillary information in the field could be a solution to cope with these difficulties. As a result, an alternative indirect approach developing pedotransfer functions (PTFs) to link hydraulic properties to ECa could be a way forward to estimate the spatial distribution of hydraulic conductivity over the whole

field. ECa measurements with electromagnetic induction (EMI) is extensive, less expensive, non-destructive, more efficient, reliable and fast, which could improve the spatial and temporal estimation of some soil properties at different scales and depths (Corwin and Lesch, 2005, Segal, et al., 2008, Sudduth, et al., 2005). In addition, for precision management, higher resolution quantification of ECa from EMI (Hedley, et al., 2013) provides an opportunity to complement the limited density of direct soil samples (Saey, et al., 2009) and to describe soil hydraulic properties with a higher resolution. Moreover, the soil ECa dataset can be used to guide sampling more effectively and efficiently (Carroll and Oliver, 2005, Corwin and Lesch, 2005).

Soil ECa appears to be a function of a variety of soil properties including soil water content, bulk density, texture, salinity, organic matter content, cation exchange capacity (CEC), and soil layer thicknesses (Corwin and Lesch, 2005, Sudduth, et al., 2013). The same parameters affecting ECa affect soil physical and hydraulic properties especially hydraulic conductivity,  $K$  (Doussan and Ruy, 2009, Sudduth, et al., 2005). Therefore, ECa can be an indirect indicator of hydraulic properties. Hydrologists, soil scientists and petroleum engineers have attempted to find out correlations between ECa and hydraulic properties (Archie, 1942, Chaplot, et al., 2011, Cosentini, et al., 2012, Doussan and Ruy, 2009, Friedman, 2005, Huntley, 1986, Lesmes and Friedman, 2005, Morin, et al., 2010, Mualem and Friedman, 1991, Purvance and Andricevic, 2000, Segal, et al., 2008, Slater, 2007) but most of them rely on laboratory experiments.

## ***1.2 Aim of the research and research strategy***

The objective of the PhD is to develop and test methods for optimizing irrigation efficiency using a combination of sensors and process based soil hydrological models. Sensors that will be used are soil moisture sensors and online tensiometers that measure water content and water potential in a fully automated field setup for quantitatively identifying flow processes in an agriculture soil. The monitoring data are continuously used to improve the model predictions of water status in the plant root zone and therefore the steering of the irrigation. We will develop and test methods for irrigation management purposes, which are extremely relevant for arid and semi-arid conditions, such as Iran, but also for the management of intensively used agricultural fields in West- and Southern Europe suffering from summer droughts related to climate change.

The specific objectives are to:

- 1) Simulate the root water uptake in vadose zone and status of water in rhizosphere (including concentrations of solutes and nutrients or pollutants) using the Hydrus-1D model in combination with other state of the art crop based models like AquaCrop
- 2) Upscale and determine soil hydraulic properties based on soft data and transfer methods
- 3) Investigate the tempo-spatial variability of soil hydraulic properties
- 4) Improve irrigation management using sensors and models for water flow and redistribution in soils.

## ***1.3 Summary of the research of the past year***

The original study site was further investigated and the modelling exercise refined. In 2011, soil samples had already been taken at eight locations and two depths 25 and 75 cm (traditional sampling strategy) to determine soil hydraulic and some other basic soil

properties. Then in 2013, at 21 locations within the field, duplicate undisturbed (100 cm<sup>3</sup> Kopecky rings) soil samples to determine the soil hydraulic properties, and one disturbed sample to measure soil properties such as texture, dry bulk density and organic matter, were taken from the of the Ap horizon. The selection of sampling locations was done by combining a design-based and model-based sampling strategy to account for the maximum variation in soil properties based on a geophysical survey with an EM38 proximal sensor (Geonics Ltd, Ontario, Canada).

K<sub>s</sub> was determined using a constant head laboratory permeameter (M1-0902e, Eijkelkamp Agrisearch Equipment, Giesbeek, the Netherlands). The soil water retention curve, (SWRC,  $\theta(h)$ ), was determined using the sandbox method (Eijkelkamp Agrisearch Equipment, Giesbeek, the Netherlands) up to a matric head of -100 cm and the standard pressure plate apparatus (Soil moisture Equipment, Santa Barbara CA, USA) for matric heads equal to or below -200 cm, following the procedure outlined in (Cornelis et al., 2005). The bulk density was obtained by drying volumetric soil samples (100 cm<sup>3</sup>) at 105 °C. Soil texture was determined using the pipette method for clay and silt fractions and sieving method for sand particles (Gee and Bauder, 1986). The organic matter content was determined by the Walkley and Black method (Walkley and Black, 1934). Soil hydraulic properties were determined according to the van Genuchten (1980) and Mualem (1976) conductivity model (MVG model) using the RETC program for Windows, version 6.02 (van Genuchten, et al., 1991).

Also the modeling of water flow for this field was further refined. Simulation of water flow and root water uptake of the field for two growing seasons (from 1 Mar. until 25 Nov. 2012-2013) was carried out by using Hydrus 1D version 4.16. The 150 cm depth of soil profile and two layers (0-34 cm, and 34 cm to 150 cm) with different material properties were chosen a priori based on field observations of layering. Based on field observations, a linear root distribution was assumed (maximum density up to 6 cm and linearly decreasing from 6 to 34 cm, no roots below 34 cm). The upper boundary condition for water flow was atmospheric (rainfall and reference evapotranspiration, E<sub>To</sub>) with surface runoff. E<sub>To</sub> was initially used without adjusting the crop coefficient because the grass at our site did not differ much from the reference crop. The Feddes model (Feddes, et al., 1977) without solute stress was used for root water uptake. Default values for grass (Taylor and Ashcroft, 1972) provided with Hydrus 1D were used.

To reduce the number of parameters of optimization and finalize the calibration process, local SA was conducted by calculating the central total parameter relative sensitivity “CTRS”. According to the results  $\alpha$ ,  $n$  and  $K_s$  are most sensitive (in decreasing order) and the sensitivity changed over time with the seasonal changes in water status in both soil layers.

In next step of the modeling approach, a period between 1 Mar. 2012 (0000 h) and 25 Dec. 2012 (2300 h) was chosen as the calibration period. We used a time interval of two hours, resulting in 12960 soil water content records based on hourly precipitation and evaporation input data. In the calibration, we optimized only the values of the most sensitive parameters ( $K_s$ ,  $n$ , and  $\alpha$ ) of the two layers, taking initial values of hydraulic parameters for each layer equal to the values estimated in the previous step (RETC program), while keeping the insensitive hydraulic parameters ( $\theta_s$ ,  $\theta_r$ ) fixed to the measured values. To avoid non-uniqueness of the parameter sets (Šimůnek and Hopmans, 2002), 37 parameter optimization scenarios were selected and analyzed for correlations among optimized parameters, i.e., optimizing six parameters (1 scenario purposed by SA), four parameters (9 scenarios), three parameters (18 scenarios) and two parameters (9 scenarios). Finally, the best performing parameter set was selected for validation using independent data from 2013 (from 1 Mar. until 12 Sep. 2013). Results showed changes in soil water content are affected mainly by the saturated hydraulic conductivity of the soil  $K_s$ , and the shape parameters of MVG parameters



$n$  and  $\alpha$ . The effect of soil hydraulic parameters were most pronounced in dry periods. The best performing parameter optimization scenario was a 2-parameter scenario with  $K_s$  optimized for each layer. The results showed a better identifiability of the parameters (less correlations among parameters) with equal performance as compared to three, four or six parameter optimization.

More work was done on developing relationships between soil hydraulic properties and ECa in order to be able to upscale measured soil hydraulic properties to the field scale. Statistical analysis for all soil samples were performed on the hydraulic and physical parameters. The mean (m), minimum and maximum (min and max), median and standard deviation (SD) of soil properties and ECa surveys were calculated. The Pearson correlation coefficient was computed between ECa and soil hydraulic data. All statistical analyses were performed using SPSS Version 19. Hydraulic parameters  $K_s$ ,  $n$  and  $\alpha$  have been log-transformed to get a normal distribution. The use of DUALEM and EM38, MVG parameters and Archie's law was investigated to derive predictive models for hydraulic properties. Two predictive modelling approaches were developed and compared to explain observed value of hydraulic parameters i.e. i) a simple regression approach and ii) applying Archie's laws for saturated and unsaturated conditions in combination with MVG equation. In a first approach we just focused on the relation between  $K_s$  and calculated  $S_e$  and FF. The latter unsaturated  $K(S_e)$  was estimated by a combination of MVG and Archie's second law equations. In that part, ECa was estimated based on  $S_e$  measured from water retention curve data. Then the water retention curve was translated to  $ECa(S_e)$  and  $ECa(h)$  functions. Due to a lack of information/measurements about the unsaturated hydraulic conductivity,  $K(h)$ , the RETC software was used to predict  $K(h)$  and  $K(S_e)$ . Finally  $K(h)$  was translated to  $ECa(h)$ . In a nutshell, we derived a simple strong relationship between  $\log K_s$  and ECa measured with DUALEM ( $r^2 \geq 0.70$ ) and ECa measured with EM38 ( $r^2 > 0.46$ ) sensors. The water retention curve can be translated to  $ECa(h)$  and  $ECa-S_e$  by combining the MVG equation and Archie's law. Results show that reformulating the MVG equation based on  $ECa-S_e$  relationships can help to estimate unsaturated hydraulic conductivity. Therefore it helps to understand flow and fluxes in an entire field in modeling approaches.

A second study site has been selected and monitoring equipment was installed in the field at two locations in collaboration between VITO and Wageningen university (WUR). At this potato field, also a combination of field monitoring and modeling (hydrological and crop based models) will be used to estimate hydraulic properties and predict water content distribution, water flow, crop yield and root water uptake at the field scale in a two layered sandy soil for irrigation management and possibly for N or pesticide leaching purposes.

## Chapter 2 Report of the past period

### 2.1 Achieved Results

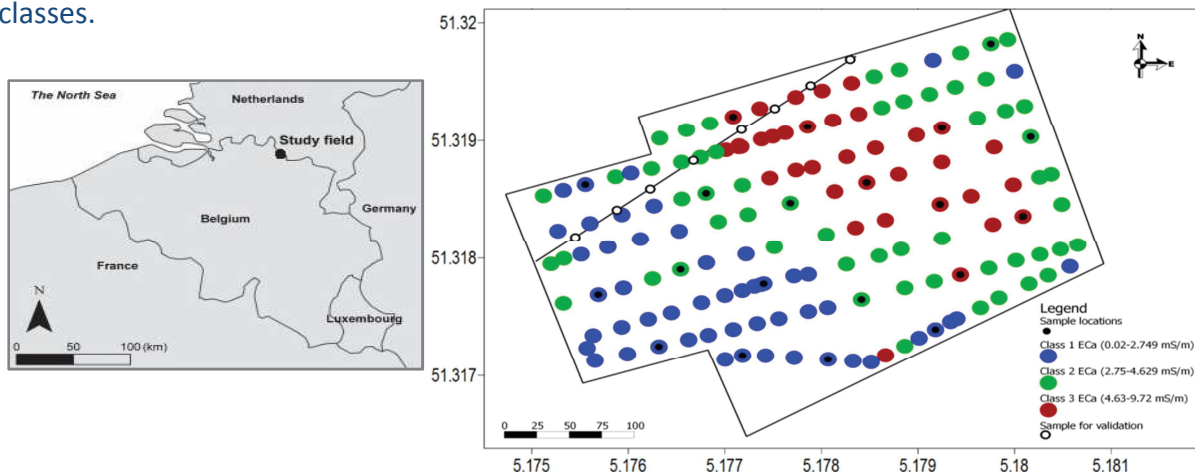
#### 2.1.1 Further characterisation of study site 1 and soil



Figure 1 shows the soil profile of the site 1. A uniform dark brown layer of sand (Ap horizon) with higher organic matter content was situated from the surface to a depth of about -33 cm, followed by a yellowish to white sand including stones and gravels (-33 to -70 cm, C1 horizon). The deeper profile from -70 to -135 cm was light gray sand (C2 horizon) including more stones and gravels (max 20%) with the similar hydraulic properties of C2 horizon. Maximum grass root density was situated from the soil surface to about -6 cm and decreased from -6 to -34 cm. The properties of the two layers of the soil profile are summarized in Table 1. Figure 2 shows the map of the classified site with Fuzzme and the 20 soil sampling locations, and 8 additional locations along transect (traditional sampling strategy).

**Fig. 1. Two-layered typical soil profile of the field close to the location of the sensors.**

The topsoil mean  $K_s$  value was 5.94, 2.87 and 2.14  $\text{cm.h}^{-1}$  for soil class 1, 2 and 3 respectively. The hydraulic conductivity shows a coefficient of variation CV of 58.36%, 49.37%, and 67.49%, in the topsoil of classes 1, 2, and 3, respectively. The average of the MVG parameter  $n$  was 2.15, 2.10, and 1.72, and  $\alpha$ , was 0.015, 0.011, and 0.011 ( $\text{cm}^{-1}$ ) for the first layer of the first, second and third class respectively. The  $n$  and  $\alpha$  values of topsoil were less than the corresponding values of each class' subsoil. The corresponding air entry value varied from 48 to 91 cm for sub and topsoils, which is higher than the value of typical sandy soils (20 to 32 cm). From fitting retention data,  $\theta_s$  ( $0.39 \text{ m}^3 \text{ m}^{-3}$ ) was almost equivalent to the porosity ( $0.38 \text{ m}^3 \text{ m}^{-3}$ ) estimated from mean bulk density (fitted values were estimated well) in topsoil of all classes.



**Fig. 2. Location and the map of the classified study site with Fuzzme and the 20 soil sampling locations with the ESAP software and additional 8 sample locations along transect.**

**Table 1. Average of soil properties of entire field for each soil class. Number between parentheses represents the coefficient of variation (CV %).**

	Class	Number of samples	Average first layer depth	GWL	$K_s$	$\theta_r$	$\theta_s$	$\alpha$	$n$	OC	Sand	Silt	Clay	$\rho_b$
			cm	cm h <sup>-1</sup>		cm <sup>3</sup> cm <sup>-3</sup>		cm <sup>-1</sup>		%	%	%	%	g cm <sup>-3</sup>
Topsoil	1	16	39 (21.14)	-136 (6.29)	5.94 (58.36)	0.08 (18.22)	0.39 (6.19)	0.015 (41.61)	2.15 (24.68)	2.12	91.48	7.12	1.4	1.60
	2	12	38 (9.55)	-109 (10.28)	2.87 (49.37)	0.09 (10.70)	0.38 (2.19)	0.011 (19.76)	2.10 (17.19)	2.17	91.13	7.32	1.55	1.62
	3	14	44 (11.89)	-87 (8.51)	2.14 (67.49)	0.08 (28.24)	0.38 (4.98)	0.011 (24.92)	1.72 (13.63)	2.15	90.01	8.06	1.93	1.60
Subsoil	1	7	39 (21.14)	-136 (6.29)	4.63 (59.52)	0.05 (47.07)	0.34 (11.10)	0.019 (23.12)	2.48 (29.41)	0.84	93.19	5.57	1.24	1.68
	2	2	38 (9.55)	-109 (10.28)	4.55 (67.94)	0.03 (0.01)	0.33 (6.06)	0.019 (1.89)	2.82 (2.62)	0.41	95.5	2.85	1.65	1.71
	3	3	44 (11.89)	-87 (8.51)	1.59 (33.05)	0.07 (61.64)	0.35 (12.34)	0.021 (64.32)	2.4 (28.12)	1.14	93.17	4.62	2.21	1.54

### 2.1.2: Soil hydrological model for a 2-layered sandy soil for irrigation management

#### 2.1.2.1 Effect of the Bottom Boundary Condition and Parameter Uncertainty on Model Prediction

A manual SA was conducted by applying various bottom boundary conditions related to the position of the GWL. In the free drainage condition, soil water content is generally underestimated especially at deeper observation nodes (Fig. 3). The results show a constant head boundary condition yields a much better agreement between the model and the observations due to wetter conditions in the lower part of the profile. The best constant head condition was in agreement with GWL observations in 2012 and 2013 (-140 and -135 cm respectively) at the location of the sensor (2012: RMSE=0.019,  $C_e$ =0.22, and  $r^2$ =0.42; 2013: RMSE=0.027,  $C_e$ =0.22 and  $r^2$ =0.40 on average). Decreasing the GWL to 120 cm overestimated the soil water content, especially at the three deepest observation nodes. The results clearly show the great importance of the bottom boundary condition in estimating soil water content in the soil profile, even for this sandy soil.

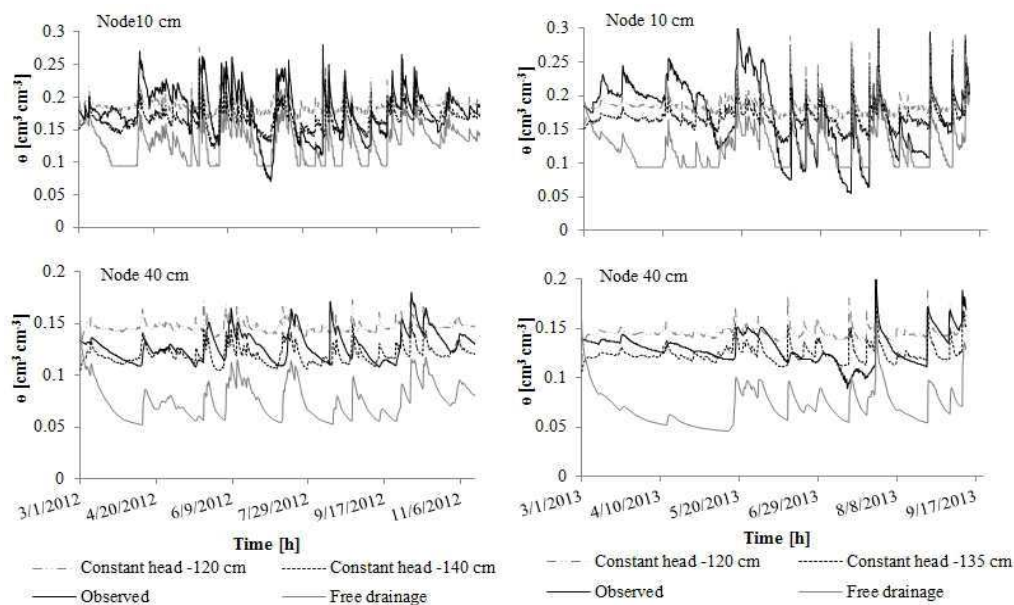


**Fig. 3: Water content estimations at 10 and 40 cm depths using the uncalibrated model for free drainage and different constant head bottom boundary conditions at the soil moisture sensor location.**

Therefore, before optimizing hydraulic model parameters, the effect of the boundary conditions should be assessed and the appropriate boundary conditions should be used.

To assess the effect of the variability in measured soil hydraulic properties on the calculated soil water content, Hydrus 1D was run 21 times using different parameter sets, soil layering and boundary conditions at each of the 21 locations. The results show that field scale variations in soil water content can be very large, due to variations in GWL and in hydraulic parameters. Our results (relatively high standard deviation) suggest that uniform water distribution using sprinkler irrigation may not be optimal, since the large variation in hydraulic properties calls for a distributed irrigation scheme.

### **2.1.2.2: Model Calibration**

Hydrus 1D was run inversely using time series of soil water content with values for  $\alpha$ ,  $n$  and  $K_s$  being optimized for the two layers (i.e., six-parameter optimization scenario). A significant correlation exists between  $\alpha$  and  $K_s$  for both layers (layer 1:  $r = 0.87$ ; layer 2:  $r = 0.95$ ) and between  $n$  and  $\alpha$  ( $r = -0.99$ ) within each layer, but not between different layers. On the other hand, there is a significant correlation between  $n$  and  $K_s$  for both layers (layer 1:  $r = -0.87$ ; layer 2:  $r = -0.94$ ). This means that  $\alpha$ ,  $n$ , and  $K_s$  within a layer cannot be determined independently and multiple solutions exist for different combinations of  $\alpha$ ,  $n$  and  $K_s$ . The high correlation between optimized parameters within a layer leads to a large uncertainty of the final parameter estimates. To avoid non-uniqueness of the inverse solution, 36 systematic four-, three- and two-parameter optimizations were conducted. All optimizations resulting in correlations among the optimized parameters were removed and only the best optimization scenarios with the uncorrelated parameters were kept. This resulted in parameter values as shown in Table 2 for a constant head corresponding to a GWL of -140 cm. For comparison purposes, only the best performing optimization with two parameters is presented for other boundary conditions (GWL = -120 cm, free drainage). A two parameter optimization (optimizing only  $K_s$  in both layers) performs equally well as compared to a six-, four- or three-parameter scenario for all performance criteria and observation depths, except a slightly smaller Nash Sutcliffe  $C_e$ . However, parameters in the six parameter scenario are considered unidentifiable due to their correlations. In this case, the model was not able to find a global minimum but found a local minimum (Marquardt-Levenberg method) due to high dimensionality of the problem and the uncertainty of the optimized values is large.

Large differences in model performance were obtained for free drainage and constant head conditions (Table 3). The model with a constant head clearly outcompetes the free drainage model. After optimization,  $R^2$  for different constant head conditions and various optimization scenarios were similar while  $C_e$  and RSME were different. Overall, the performance of the model to predict soil water content at 40 cm was less as compared to the other observation depths. The model performs well for the 10, 20, and 30 cm depths where the plant roots are concentrated and which are consequently the most critical in terms of irrigation optimization.

The two parameters scenario requires less parameters (one parameter for each layer) to be optimized, performs better as compared to the uncalibrated model (Table 3 and Fig. 3 5) and is therefore to be preferred. Large confidence limits indicate uncertain estimations of a particular parameter (Šimůnek and Hopmans, 2002). The optimized  $K_s$  with 95% confidence limits (CL) for the first and second layer were 1.71 (1.64 – 1.78), and 3.09 (2.96 – 3.22)  $\text{cm} \cdot \text{h}^{-1}$ , respectively in two parameters scenario with -140 cm GWL. Therefore, this optimization result was considered the best and chosen for the validation run.

**Table 2. Optimized values of parameters for the best (out of 37) optimization scenarios yielding uncorrelated parameter sets. Values indicated in *italic* are values fixed to the measured values close to the sensor location. Number between parentheses represents the standard errors of optimized parameter.**

Boundary condition	Number of optimized parameters	First material			Second material		
		$\alpha_1$ (cm <sup>-1</sup> )	$n_1$	$K_{s1}$ (cm h <sup>-1</sup> )	$\alpha_2$ (cm <sup>-1</sup> )	$n_2$	$K_{s2}$ (cm h <sup>-1</sup> )
Constant head (-140 cm)	4	<i>0.017</i>	2.59 (3.26x10 <sup>-3</sup> )	1.98 (3.76x10 <sup>-2</sup> )	0.019 (5.24x10 <sup>-5</sup> )	<i>2.34</i>	2.01 (4.29x10 <sup>-2</sup> )
	3	<i>0.017</i>	2.72	1.90 (3.59x10 <sup>-2</sup> )	0.019 (5.21x10 <sup>-5</sup> )	<i>2.34</i>	2.26 (4.58x10 <sup>-2</sup> )
	2	<i>0.017</i>	2.72	1.71 (3.61x10 <sup>-2</sup> )	0.021	<i>2.34</i>	3.09 (6.53x10 <sup>-2</sup> )
Constant head (-120 cm)	2	<i>0.017</i>	2.72	2.11 (7.82x10 <sup>-2</sup> )	0.021	<i>2.34</i>	0.82 (1.25x10 <sup>-2</sup> )
	2	<i>0.017</i>	2.72	0.99 (3.18x10 <sup>-2</sup> )	0.021	<i>2.34</i>	0.33 (6.21x10 <sup>-3</sup> )

### 2.1.2.3: Model Evaluation

The validation results (with the same parameters values as the calibration period) under different upper (rainfall, ET) and lower (groundwater depth, e.i. -135 cm) boundary conditions, show that the model performs less well at all observation depths (Fig. 4, Table 3). Specifically, soil water content is underpredicted during summer months (June-August) and overpredicted during winter and spring. These probably caused by different upper (rainfall and irrigation) and bottom boundary conditions (different GWL) and different water flow process. To which extent this affects the calculated irrigation requirements, is shown in the subsequent section.

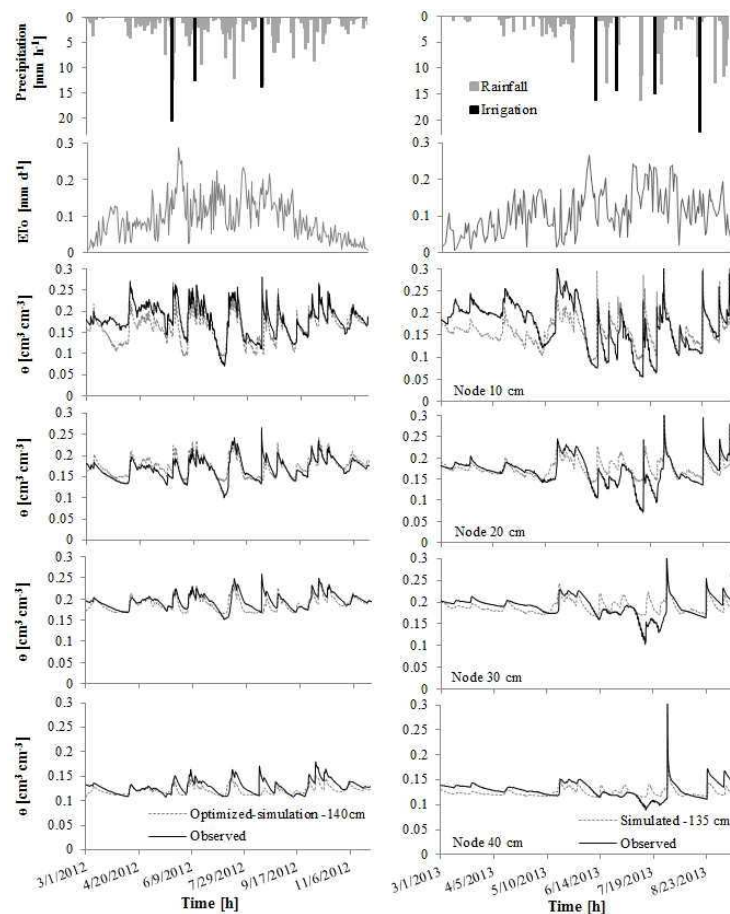


**Fig. 4. Observed and simulated time series of soil water content with inverse modeling for the selected best optimization scenario for 2012 and validation results of 2013 from best performing optimized parameters (scenarios 2 parameters -140 cm GWL).**

**Table 3. Calculated performance criteria describing the correspondence between measured and simulated soil water content for each optimization scenario under different boundary conditions.**

	Boundary condition	Number of optimized parameters	Nodes depth	RMSE †	C <sub>e</sub> †	R <sup>2</sup> †
			cm			
Uncalibrated (2012)	Constant head (-140 cm)	---	10	0.029	0.33	0.55
			20	0.018	0.42	0.51
			30	0.016	0.18	0.36
			40	0.014	-0.05	0.26
	Constant head (-120 cm)	---	10	0.032	0.2	0.36
			20	0.039	-1.66	0.26
			30	0.029	-1.65	0.16
			40	0.023	-1.76	0.08
	Free drainage	---	10	0.05	-1.41	0.51
			20	0.039	-1.62	0.7
			30	0.057	-9.3	0.6
			40	0.053	-14.27	0.61
Calibration period (2012)	Constant head (-140 cm)	6	10	0.023	0.58	0.67
			20	0.017	0.51	0.72
			30	0.011	0.64	0.66
			40	0.009	0.58	0.58
		4	10	0.023	0.57	0.67
			20	0.017	0.52	0.73
			30	0.011	0.63	0.66
			40	0.009	0.58	0.58
	Constant head (-120 cm)	3	10	0.028	0.39	0.67
			20	0.013	0.69	0.72
			30	0.012	0.55	0.65
			40	0.009	0.56	0.57
		2	10	0.027	0.42	0.67
			20	0.014	0.67	0.73
			30	0.012	0.53	0.65
			40	0.011	0.31	0.57
	Free drainage	2	10	0.022	0.63	0.63
			20	0.031	-0.62	0.72
			30	0.024	-0.86	0.65
			40	0.019	-0.97	0.56
Validation period (2013)	Constant head (-135 cm)	2	10	0.035	0.05	0.52
			20	0.027	-0.28	0.56
			30	0.033	-2.51	0.44
			40	0.026	-2.66	0.34
			10	0.042	0.33	0.39
			20	0.025	0.40	0.44
			30	0.020	0.27	0.30
			40	0.015	0.21	0.30

†RMSE, C<sub>e</sub> and R<sup>2</sup> are the root-mean-square deviation, the Nash–Sutcliffe coefficient of efficiency (cm<sup>3</sup> cm<sup>-3</sup>) and the coefficient of determination.



#### 2.1.2.4: Effect of Optimization Scenarios on Estimated Water Stress

The calculated potential-reference evapotranspiration (ET<sub>o</sub>) values for 2012 and 2013 (same period from 1 Mar. to 12 Sep.) were 523 and 524 mm, respectively. The cumulative actual transpiration for the calibration (2012) and validation (2013) period was 490 and 496 mm, respectively. Cumulative actual fluxes across the bottom of the soil profile was 31.2 mm and 23.2 mm (upward-inflow) and the sum of irrigation and precipitation over the simulation period was 463 mm and 502 mm for 2012 and 2013 respectively. In 2013 input water was thus higher than in 2012 and water usage (capillary rise) from groundwater was less as compared to 2012. Comparing 2012 and 2013 meteorological data suggested that increasing water application with about 27 mm (Table 4) decrease the plant experience to a period of water stress which is about half as as long as 2012 (for 2012: 651 and for 2013: 368 hour). The result shows that during summer 2012 and 2013 more irrigation (around 30-50 mm) was needed in the soil class 1 area. Irrigation over more applications with application at least in June and July instead of a huge amount applied in late summer. There is a significant effect of the bottom boundary condition on the calculated water stress. A free drainage condition results in a larger number and higher duration of stress conditions (Table 4) and overestimates water stress, while a shallower imposed GWL (-120 cm) underestimates water stress. Different parameter optimization strategies (two-, three-, four- or six-parameter optimizations) do not affect the calculated water stress as significantly as does the bottom boundary. Therefore, this result suggest that a two stage optimization, i.e., firstly optimize boundary conditions and secondly optimize hydraulic parameters is needed for precision irrigation management purposes.

**Table 4: Total duration, number and extent of water stress (WS) for different boundary conditions and scenarios.**

Boundary condition	parameter fit	2012 (1 Mar. to 12 Sep)					Required irrigation amount
		Number of WS periods	Total Duration of WS	Degree of WS<90%	Irrigation amount	rainfall	
			h			mm	
Constant head (-140 cm) uncalibrated		0	0	≥1			0
Free drainage	2	7	1135	0.35	65 (3 times)	398.2	90
Constant head (-120 cm)	2	1	62	0.85			5
Constant head (-140 cm)	2	7	651	0.65			50
Constant head (-140 cm)	4	5	489	0.65			40
Constant head(-140 cm: 2012)	6	6	472	0.65			40
2013 (1 Mar. to 12 Sep)							
Constant head (-135 cm) uncalibrated		0	0	≥1			0
Free drainage	2	6	1262	0.22			100
Constant head (-120 cm)	2	2	203	0.75	89 (4 times)	413.2	15
Constant head (-135 cm)	2	4	368	0.65			30
Constant head (-135 cm)	4	2	253	0.65			25
Constant head (-135 cm: 2013)	6	2	229	0.70			20

#### 2.1.2.5: Conclusion of the 1D soil hydrological modeling

The results demonstrated clearly the profound effect of the position of the GWL, and to a lesser extent, the effect of spatially variable soil hydraulic properties ( $K_s$ ,  $n$  and  $\alpha$ ) on the estimated water content in a sandy two-layered soil under grass in a temperate maritime climate. Our results show that currently applied uniform water distribution using sprinkler

irrigation seems not to be efficient since at locations with shallow groundwater, the amount of water applied will be excessive as compared to the plant requirements while in locations with a deeper GWL, requirements will not be met.

37 optimization scenarios were conducted. Although the model was sensitive to MVG's  $K_s$ ,  $\alpha$ , and  $n$ , the most relevant optimization scenario was a  $K_s$  only optimization in each layer (less parameters with almost similar performance criteria). The agreement of the simulated moisture with observed soil moisture data in the validation period confirmed that the selected model performed adequately. Comparing the degree of water stress for different optimization scenarios of groundwater depth, showed that grass was exposed to water stress in summer in 2013 but not for such a long period as compared to the 2012 growing season. The degree of water stress simulated with Hydrus 1D suggested to increase the irrigation amount in 2012 and 2013 and at least one or two times in the summer (June and July) and further distributing the amount of irrigation during the growing season, instead of using a huge amount of irrigation later in the season, as is common practice by the farmer.

### 2.1.3: Upscaling soil saturated hydraulic conductivity using ECa

#### 2.1.3.1: Relation between soil hydraulic properties and ECa

The most significant correlation can be seen between ECa values of different sensors and depths (Table 5). There are positive and significant correlations between EM38<sub>v,100</sub>, DUALEM<sub>p,50</sub> and DUALEM<sub>p,100</sub> ( $r \geq 0.84$ ). The greatest significant correlation of hydraulic properties and electrical conductivity occurred between  $K_s$  and ECa of DUALEM ( $r \geq -0.84$ ) while there is no correlation between  $\alpha$  and all ECa values derived by different sensors. The correlation between log  $n$  and EM and DUALEM sensors at various depths were relatively strong ( $r \geq 0.43$ ;  $p \leq 0.05$ ). Results showed a stronger correlations between ECa and saturated soil water content,  $\theta_s$ , than residual water content,  $\theta_r$  especially for the DUALEM sensor. Saturated hydraulic conductivity (log  $K_s$ ) is significantly correlated to log  $n$  and log  $\alpha$  ( $r \geq 0.56$ ;  $p = 0.01$ ). There is no significant relation between the MVG transformed shape parameters log  $n$  and log  $\alpha$ . There are significant correlation between shape parameters log  $\alpha$  and the saturation water content ( $r = -0.59$ ;  $p = 0.01$ ) and residual water content ( $r = 0.44$ ;  $p = 0.05$ ).

**Table 5. Correlations between hydraulic parameters and appearant electrical conductivity.**

Variable	1	2	3	4	5	6	7	8	9	10	11	12
1 EM38 <sub>v,50</sub>	1											
2 EM38 <sub>v,100</sub>	0.92**	1										
3 DUALEM <sub>p,50</sub>	0.69**	0.84**	1									
4 DUALEM <sub>p,100</sub>	0.80**	0.93**	0.95**	1								
5 EC <sub>sat</sub>	0.30	0.31	0.21	0.24	1							
6 Log $K_s$	-0.48*	-0.68**	-0.85**	-0.84**	-0.22	1						
7 Log $\alpha$	-0.11	-0.23	-0.37	-0.37	0.01	0.57**	1					
8 Log $n$	-0.45*	-0.51*	-0.45*	-0.43*	-0.41*	0.56**	-0.17	1				
9 $\theta_r$	-0.11	-0.14	0.03	-0.023	-0.51*	0.06	-0.59**	0.60**	1			
10 $\theta_s$	-0.07	-0.31	-0.48*	-0.47*	0.04	0.43*	0.44*	-0.11	-0.11	1		
11 Sand	-0.43	-0.51*	-0.57**	-0.54*	0.01	0.56*	0.45*	0.56*	-0.09	0.10	1	
12 Porosity	0.06	-0.03	-0.15	-0.17	0.07	0.39	-0.03	0.10	0.18	0.55*	0.20	1

\*\*and \* marked correlation significant at  $P \leq 0.01$  and  $P \leq 0.05$  level respectively.



### 2.1.3.2: Approach 1: Regression estimation of hydraulic properties from ECa measurements

A higher resolution ECa dataset in combination with a limited 20 spatial point dataset ( $n=20$ ) was used to provide regression models to predict soil saturated hydraulic conductivity,  $K_s$ . Due to the small number of sampling locations i.e. 20 locations, the dataset was not split into calibration and validation set but 8 additional locations (Fig. 2) are taken into account for validation purposes. A strong negative relation between  $\log K_s$  and ECa of DUALEM sensor was obtained with a regression equation ( $r^2 \geq 0.70$ , Fig 6). The DUALEM data model gives better predictions of  $K_s$  (larger  $R^2$ ) compared to the EM38 data through regression of the data (Fig. 5). The measured versus predicted  $K_s$  for the validation dataset of regression equations are presented in Fig. 5. The results confirm that the performance of the DUALEM<sub>p,100</sub>- $K_s$  model is relatively better than that of the same sensor with 50 cm DOE and of the EM38 sensor (RMSE = 1.31 cmh<sup>-1</sup>,  $R^2 = 0.55$ ). It is therefore possible to predict  $K_s$  by using different equations for the various sensors as shown in Fig. 6.

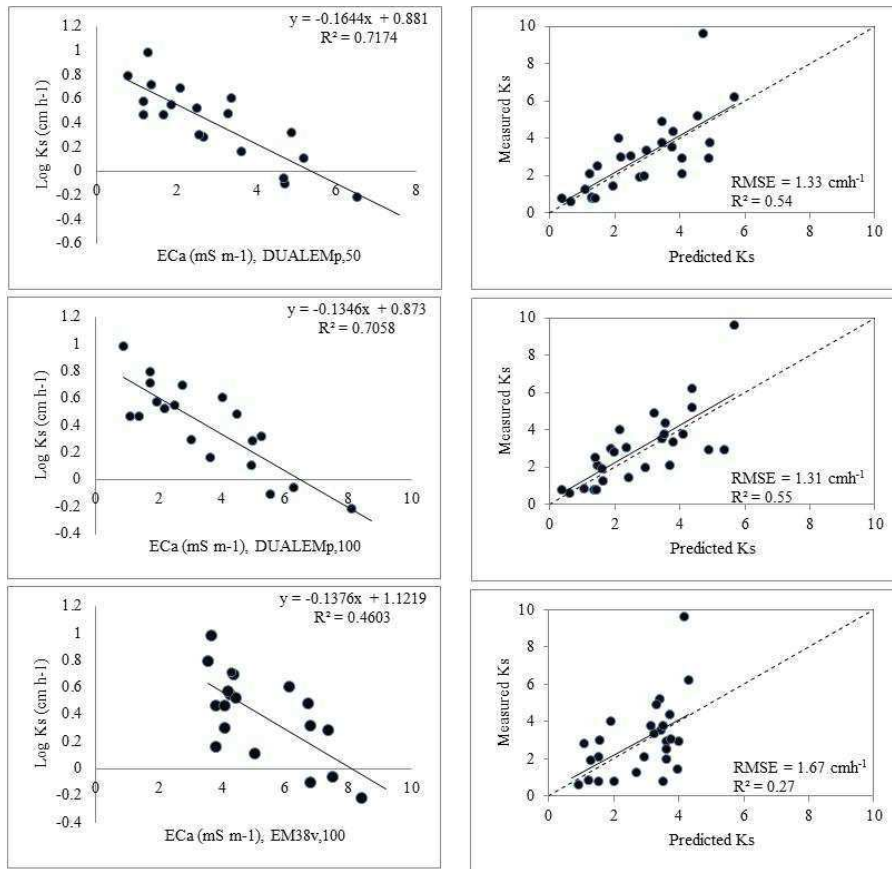


Fig. 5. Relationship between electrical conductivity measured with different sensors and laboratory hydraulic conductivity for 19 samples and measured vs. predicted saturated hydraulic conductivity for 27 locations. (EM38<sub>v,100</sub>: EM38-100cm vertical, DUALEM<sub>p,50</sub>: DUALEM-21S -50 cm perpendicular, DUALEM<sub>p,100</sub>: DUALEM-21S -100 cm perpendicular).

### 2.1.3.3: Approach 2: Unsaturated hydraulic conductivity estimates from ECa

Soil water potential as function of degree of saturation is depicted in Fig 6a. The soil water retention was not very low (27.6% at -100 cm and 8.02% at -15000 cm) as in a typical sand but it sharply drops within the suction range of -100 to -150000 cm (table 1 and figure 6a). Applying Archie's second law to the water retention curve with average values of the shape parameters of MVG (table 1) leads to the following equation (Eq. 1):

$$S_e(h) = \sqrt{\frac{EC_a}{12.047}}(h) = 1 + (|0.012h|^{1.93})^{-0.482} \quad (1)$$

Variation of ECa with the water content (water saturation) and the fit to MVG-Archie equation (Eq. 1) is shown in Fig. 6b. The slope of the ECa-water saturation changes for lower than ~0.28 % of saturation (~-320 cm) because of a water film forming over the solid surface (Doussan and Ruy, 2009, Movahedi Naeini and Rezaei, 2009). Due to the sandy texture of our soil, low values of ECa are found for suctions lower than -320 cm (Fig. 6c).

The hydraulic conductivity-water potential function  $K(h)$ , fitted to the MVG equation is shown in figure 7a. Fitting MVG with the average of measured hydraulic parameters  $K_s$ ,  $n$  and  $\alpha$  results in Eq. 2 as:

$$K(S_{e(h)}) = 3.19 \left( \sqrt{\frac{ECa}{12.047}} \right)^{0.5} \left[ 1 - \left( 1 - \left( \sqrt{\frac{ECa}{12.047}} \right)^{2.075} \right)^{0.482} \right]^2 \quad (2)$$

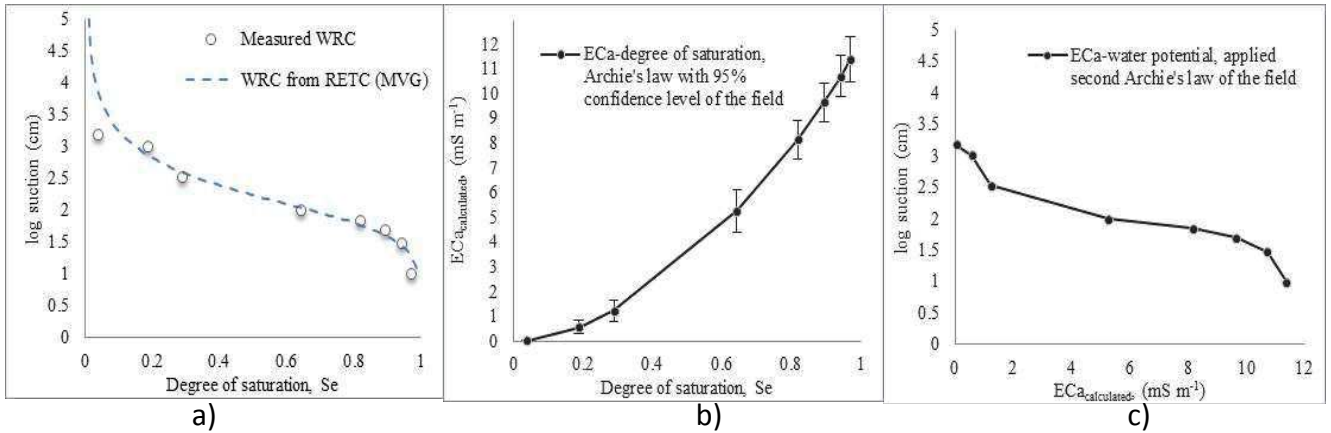


**Fig. 6.** Measured water potential as function of degree of saturation (solid points) and estimated MVG parameters by RETC program (dashline) (a), calculated ECa based on Archie's second law as a function of degree of saturation. Bars represent  $\pm 95\%$  confidence level of duplicate samples (b) and ECa water potential function (c).

Figure 7b shows the hydraulic conductivity variation with ECa as given by equation 2. It demonstrates that field ECa measurements can help to estimate hydraulic conductivity. To verify the K-ECa relation results of this study it is necessary to carry out lab experiments and more investigations in different fields and soil types.

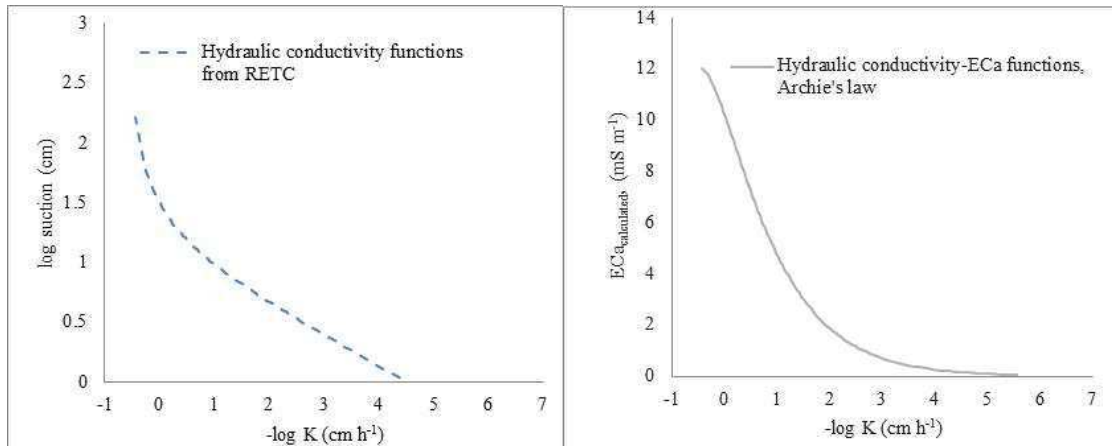


**Fig. 7.** Unsaturated hydraulic conductivity-matric head functions,  $K(h)$ , (from RETC) and ECa-unsaturated hydraulic conductivity function for the entire field,  $K(ECa)$ , (Eq. 2).

## **2.2: Scientific in- and output**

### **Courses and workshops**

- Aquacrop workshop from Monday 16th to Friday 20th July 2012 at KU Leuven University, by Dirk Raes.
- ENVITAM course on HP1 (HYDRUS + PHREEQC). From 25th to 28th March 2013 at Gent University (Faculty of Bioscience Engineering), by Diederik Jacques.
- Contaminant transport in soil, second semester 2012-2013, Gent University, by Prof. Piet Seuntjens.
- Soil physics, first semester 2012-2013, Gent University (Faculty of Bioscience Engineering), by Prof. Wim Cornelis.
- Land information system, second semester 2012-2013, Gent University (Faculty of Bioscience Engineering), by Prof. Ann Verdoodt.
- Intermediate academic English course, first semester 2012-2013, Gent University, by university language center (UTC).
- Advanced Academic English: Conference Skills - Presentation Skills in English, first semester 2013-2014 Gent University, by university language center (UTC).

### **Publications**

#### **Journals:**

Rezaei, M., P. Seuntjens., I. Joris, W. Boënné, S. Van hoey., W. Cornelis. 2014. Sensitivity analysis of a soil hydrological model for estimating soil water content in a two-layered sandy soil for irrigation management purposes. Vadose zone Journal. Submitted 14 May 2014.

Rezaei, M., P. Seuntjens., I. Joris, W. Boënné., W. Cornelis. 2014. Upscaling and predicting hydraulic properties using apparent electrical conductivity in a sandy grassland for precision agriculture. Under revision.

#### **Conference proceeding:**

Rezaei, M., P. Seuntjens., I. Joris, W. Boënné, S. Van hoey., W. Cornelis. 2013. Optimizing Hydrus 1D for irrigation management purposes in sandy grassland. In proceeding of: The 2nd European Symposium of Water Technology & Management, At Leuven, Belgium. pp 122-126. Poster.

Rezaei, M., P. Seuntjens., I. Joris, R. Shahidi., W. Boënné, J. De Pue., W. Cornelis. 2014. Effects of spatial variability of soil hydraulic properties on hydrological model for irrigation management purposes. In the 9th International Soil Science Congress on "The Soul of Soil and Civilization" in Side, Antalya, Turkey on October 14-17, 2014. Oral.

Rezaei, M., P. Seuntjens., I. Joris, W. Boënné, W. Cornelis. 2014. An alternative tool to predict and upscale soil saturated hydraulic conductivity: apparent soil electrical conductivity. In the 9th International Soil Science Congress on "The Soul of Soil and Civilization" in Side, Antalya, Turkey on October 14-17, 2014. Oral.

Rezaei, M., P. Seuntjens., I. Joris, W. Boënné, W. Cornelis. 2014. Estimation of the spatial distribution of soil hydraulic characteristics using apparent soil electrical conductivity as proxy data. In TERENO international conference 2014. In Boon, Germany on 29<sup>th</sup> September-2<sup>nd</sup> October 2014. Submitted.

## Chapter 3: Future perspectives

### 3.1 Evaluation of the results and currently missing elements

The dataset now consists of data for two growing seasons for grassland. In the coming months a quasi 3D model will be set up for this data set with a combination of Hydrus 1D and the Lingra-N crop based model (Wolf, 2012). Also a second field has been selected and monitoring equipment were installed in the field at two locations in collaboration between VITO and Wageningen university. At the second field, again a combination of field monitoring and modeling will be used to estimate hydraulic properties and predict water content distribution, water flow and root water uptake at the field scale in a two layered sandy soil for irrigation management and possibly for N or pesticide leaching purposes.

The objectives of the study at the second field are to:

- a)** Evaluate the PTFs (Eca-Ksat) of the previous field study to investigate the variability of hydraulic properties at the new field site and validate the equations;
- b)** Carry out the previous systematic methodology in modeling approach to predict water content distribution, water flow and root water uptake of potato with Hydrus 1D and crop yield with AquaCrop model (crop based model);
- c)** Investigate and simulate the fate of applied fertilizer (N) and/or contaminants (pesticide) in soils (leaching) (still under discussion with WUR).

In the field, monitoring equipment has been installed in Spring (11 Apr. 2014). A short description of the installation is given below:

**Sensors locations:** based on EMI survey, GWL and field condition and survey we determined the locations where the sensor were installed (Fig. 8).

#### **Setup field monitoring system:**

- *At first location (1: 51.310885°, 5.165263°):*
  - One weather station (type CM10, Campbell Scientific Inc., Utah, USA).
  - One soil water content profile probe (type EasyAG50, Sentek Technologies Ltd., Stepney, Australia), to measure soil-water content at 10, 20, 30, 40 and 50 cm depths.
  - Two tensiometers (type T4e, UMS, Munich, Germany) at depths of 20 and 40 cm.
  - A diver to measure the ground water fluctuations at location.
- *At second location (2: 51.312237°, 5.168495°):*
  - One soil water content profile probe (type Dacom, The Netherlands), to measure soil-water content at 10, 20, 30, 40, 50 and 60 cm depths.
  - A diver, to measure the ground water fluctuations at each location.

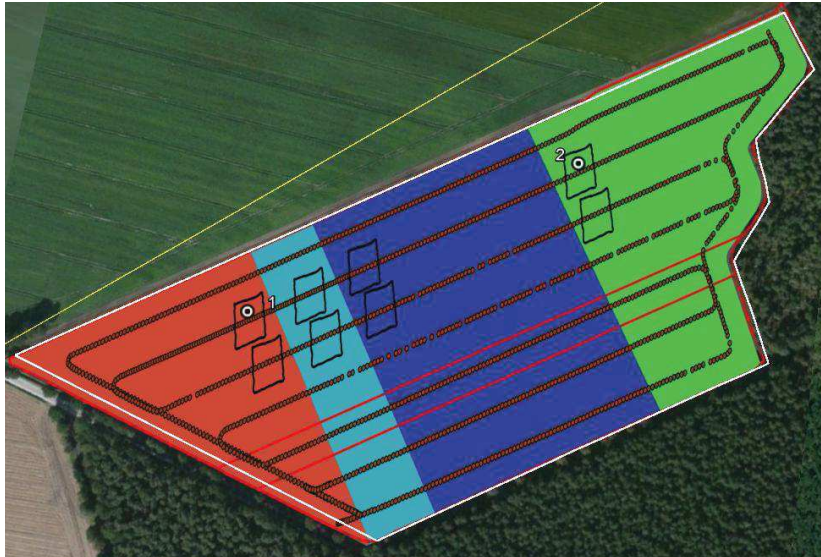


**Fig. 9. A map of the site 2 and locations of sensors. The colours show different zones according to compost application (red: 10 to Green: 50 ton/ha compost application)**

### ***3.2 Planning***

Reporting is done to Ghent University, Vito and the Ministry of science, research and technology of Iran. Below is an updated work schedule for the four year period (table 6) and the status for May 2014.

Table 6: Overview of working schedule

<Meisam Rezaei>		Actualised working schedule on <23.5.2014>															
Started on <15.02.2012>																	
Task 1	<b>Literature Review, existing data analysis and work plan</b>																
	literature review: models, processes, inverse modeling, data assimilation methods, ECa, Penetrometer																
	data analysis existing data field site at Vandenborne site 1 and 2																
	GIS analysis field data and point-to-field extrapolation of hydraulic properties (in collaboration with UGhent)																
	Finding relationship between soil properties and available data (correlation and regression)																
	completing proposal writing work plan																
Task 2	<b>Parameter estimation and model calibration</b>																
	manual calibration of historical data set																
	inverse optimisation using Hydrus																
Task 3	<b>Modelling</b>																
	setup 1D hydrological models for individual soil columns																
	root distribution, plant uptake and ET- Crop based modeling																
	setup quasi 3D hydrological model (parallel columns) for the field site at Vandenborne																
	Application of methods to include weather forecast and sensor data in predictions on water flow																
Task 4	<b>Field work and additional collection of data</b>																
	Installation of new sensor																
	Checking the data set and equipments twice to four times a month																
	Soil description and delineation of groundwater depth- soil sampling																
	Laboratory analysis																
Task 5	<b>Reporting</b>																
	Draft paper on the modelling ....																
	Draft a paper ECa data set																
	take a note and writing a draft of thesis																
	Journal and conference paper																
Task 6	<b>Doctoral education</b>																
	Speciall courses and summer school courses																
	English language and writing course																

Legend: (The vertical green line indicates the end of the present quarter)

Planning starting doctorate
  Finished
  Not planned, additional quarters
  Planned but not realised



## References

- Abbasi, F., J. Feyen and M.T. van Genuchten. 2004. Two-dimensional simulation of water flow and solute transport below furrows: model calibration and validation. *J Hydrol* 290: 63-79. doi:10.1016/j.jhydrol.2003.11.028.
- Abbasi, F., J. Simunek, J. Feyen, M.T. van Genuchten and P.J. Shouse. 2003. Simultaneous inverse estimation of soil hydraulic and solute transport parameters from transient field experiments: Homogeneous soil. *T Asae* 46: 1085-1095.
- Akhtar, F., B. Tischbein and U.K. Awan. 2013. Optimizing deficit irrigation scheduling under shallow groundwater conditions in lower reaches of Amu Darya river basin. *Water Resour Manag* 27: 3165-3178. doi:10.1007/s11269-013-0341-0.
- Archie, G.E. 1942. The Electrical Resistivity Log as an Aid in Determining Some Reservoir Characteristics. *Transactions of the American Institute of Mining, Metallurgical and Petroleum Engineers* 146: 54-62. doi:10.2118/942054-G.
- Brutsaert, W. 2005. *Hydrology, An Introduction* Cambridge University Press, Cambridge, United Kingdom.
- Cannavo, P., J.M. Harmand, B. Zeller, P. Vaast, J.E. Ramirez and E. Dambrine. 2013. Low nitrogen use efficiency and high nitrate leaching in a highly fertilized *Coffea arabica*-*Inga densiflora* agroforestry system: a N-15 labeled fertilizer study. *Nutr Cycl Agroecosys* 95: 377-394. doi:10.1007/s10705-013-9571-z.
- Carroll, Z.L. and M.A. Oliver. 2005. Exploring the spatial relations between soil physical properties and apparent electrical conductivity. *Geoderma* 128: 354-374. doi:DOI 10.1016/j.geoderma.2005.03.008.
- Chaplot, V., G. Jewitt and S. Lorentz. 2011. Predicting plot-scale water infiltration using the correlation between soil apparent electrical resistivity and various soil properties. *Phys Chem Earth* 36: 1033-1042. doi:DOI 10.1016/j.pce.2011.08.017.
- Cornelis, W.M., M. Khlosi, R. Hartmann, M. Van Meirvenne and B. De Vos. 2005. Comparison of unimodal analytical expressions for the soil-water retention curve. *Soil Sci Soc Am J* 69: 1902-1911. doi:10.2136/sssaj2004.0238.
- Corwin, D.L. and S.M. Lesch. 2005. Characterizing soil spatial variability with apparent soil electrical conductivity I. Survey protocols. *Comput Electron Agr* 46: 103-133. doi:10.1016/j.compag.2004.11.002.
- Cosentini, R.M., G. Della Vecchia, S. Foti and G. Musso. 2012. Estimation of the hydraulic parameters of unsaturated samples by electrical resistivity tomography. *Geotechnique* 62: 583-594. doi:DOI 10.1680/geot.10.P.066.
- Doussan, C. and S. Ruy. 2009. Prediction of unsaturated soil hydraulic conductivity with electrical conductivity. *Water Resour Res* 45. doi:10.1029/2008wr007309.
- Ebrahimian, H., A. Liaghat, M. Parsinejad, F. Abbasi and M. Navabian. 2012. Comparison of One- and two-dimensional models to simulate alternate and conventional furrow fertigation. *J Irrig Drain E-Asce* 138: 929-938. doi:10.1061/(ASCE)Ir.1943-4774.0000482.
- Evelt, S.R., L.K. Heng, P. Moutonnet and M.L. Nguyen. 2008. Field estimation of soil water content: A practical guide to methods, instrumentation and sensor technology IAEA-TCS-30, Vienna, Austria.
- Feddes, R.A., H. Zaradny and P. Kowalik. 1977. Simulation of evapotranspiration with different root water-uptake functions. *Eos T Am Geophys Un* 58: 900-900.
- Fernández-Gálvez, J., L.P. Simmonds and E. Barahona. 2006. Estimating detailed soil water profile records from point measurements. *European Journal of Soil Science* 57: 708-718. doi:10.1111/j.1365-2389.2005.00761.x.
- Friedman, S.P. 2005. Soil properties influencing apparent electrical conductivity: a review. *Comput Electron Agr* 46: 45-70. doi:DOI 10.1016/j.compag.2004.11.001.
- Gandolfi, C., A. Facchi and D. Maggi. 2006. Comparison of 1D models of water flow in unsaturated soils. *Environ Modell Softw* 21: 1759-1764. doi:10.1016/j.envsoft.2006.04.004.
- Gee, G.W. and J.W. Bauder. 1986. Particle-size analysis. In: A. Klute, editor *Methods of soil analysis, Part 1*, 2nd edn. Soil Science Society of America, Madison. p. 383-411.

Hedley, C.B., P. Roudier, I.J. Yule, J. Ekanayake and S. Bradbury. 2013. Soil water status and water table depth modelling using electromagnetic surveys for precision irrigation scheduling. *Geoderma* 199: 22-29. doi:DOI 10.1016/j.geoderma.2012.07.018.

Huntley, D. 1986. Relations Between Permeability and Electrical Resistivity in Granular Aquifers. *Ground Water* 24: 466-474. doi:10.1111/j.1745-6584.1986.tb01025.x.

Jacques, D., C. Smith, J. Simunek and D. Smiles. 2012. Inverse optimization of hydraulic, solute transport, and cation exchange parameters using HP1 and UCODE to simulate cation exchange. *J Contam Hydrol* 142: 109-125. doi:10.1016/j.jconhyd.2012.03.008.

Jiang, S., L.P. Pang, G.D. Buchan, J. Simunek, M.J. Noonan and M.E. Close. 2010. Modeling water flow and bacterial transport in undisturbed lysimeters under irrigations of dairy shed effluent and water using HYDRUS-1D. *Water Res* 44: 1050-1061. doi:10.1016/j.watres.2009.08.039.

Jones, H.G. 2004. Irrigation scheduling: advantages and pitfalls of plant-based methods. *Journal of experimental botany* 55: 2427-2436. doi:10.1093/jxb/erh213.

Jury, W. and R. Horton. 2004. *Soil Physics*. 6th ed. John Wiley & Sons, New York.

Lesmes, D. and S. Friedman. 2005. Relationships between the Electrical and Hydrogeological Properties of Rocks and Soils. In: Y. Rubin and S. Hubbard, editors, *Hydrogeophysics*. Springer Netherlands. p. 87-128.

Li, Y., W. Kinzelbach, J. Zhou, G.D. Cheng and X. Li. 2012. Modelling irrigated maize with a combination of coupled-model simulation and uncertainty analysis, in the northwest of China. *Hydrol Earth Syst Sc* 16: 1465-1480. doi:10.5194/hess-16-1465-2012.

Mohanty, B.P., M. Cosh, V. Lakshmi and C. Montzka. 2013. Remote sensing for vadose zone hydrology: A synthesis from the vantage point. *gsvadzone* 12: -. doi:10.2136/vzj2013.07.0128.

Morin, R.H., D.R. LeBlanc and B.M. Troutman. 2010. The Influence of Topology on Hydraulic Conductivity in a Sand-and-Gravel Aquifer. *Ground Water* 48: 181-190. doi:DOI 10.1111/j.1745-6584.2009.00646.x.

Movahedi Naeini, S.A.R. and M. Rezaei. 2009. *Soil Physics, Fundamentals and Applications*. Gorgan University of Agricultural Sciences and Natural Resources Publications, Gorgan, Iran. p. 445.

Mualem, Y. and S.P. Friedman. 1991. Theoretical Prediction of Electrical-Conductivity in Saturated and Unsaturated Soil. *Water Resour Res* 27: 2771-2777. doi:Doi 10.1029/91wr01095.

Nosetto, M.D., E.G. Jobbagy, A.B. Brizuela and R.B. Jackson. 2012. The hydrologic consequences of land cover change in central Argentina. *Agr Ecosyst Environ* 154: 2-11. doi:10.1016/j.agee.2011.01.008.

Pardossi, A., L. Incrocci, G. Incrocci, F. Malorgio, P. Battista, L. Bacci, et al. 2009. Root zone sensors for irrigation management in intensive agriculture. *Sensors-Basel* 9: 2809-2835. doi:10.3390/S90402809.

Purvanca, D.T. and R. Andricevic. 2000. On the electrical-hydraulic conductivity correlation in aquifers. *Water Resour Res* 36: 2905-2913. doi:Doi 10.1029/2000wr900165.

Richards, L.A. 1931. Capillary conduction of liquids through porous mediums. *Journal of Applied Physics* 1: 318-333. doi:10.1063/1.1745010.

Rocha, D., F. Abbasi and J. Feyen. 2006. Sensitivity analysis of soil hydraulic properties on subsurface water flow in furrows. *J Irrig Drain E-Asce* 132: 418-424. doi:10.1061/(Asce)0733-9437(2006)132:4(418).

Sadeghi, M. and S.B. Jones. 2012. Scaled solutions to coupled soil-water flow and solute transport during the redistribution process. *Vadose Zone J* 11. doi:10.2136/Vzj2012.0023.

Saey, T., M. Van Meirvenne, H. Vermeersch, N. Ameloot and L. Cockx. 2009. A pedotransfer function to evaluate the soil profile textural heterogeneity using proximally sensed apparent electrical conductivity. *Geoderma* 150: 389-395. doi:10.1016/j.geoderma.2009.02.024.

Satchithanantham, S., V. Krahn, R. Sri Ranjan and S. Sager. 2014. Shallow groundwater uptake and irrigation water redistribution within the potato root zone. *Agr Water Manage* 132: 101-110.

Segal, E., S.A. Bradford, P. Shouse, N. Lazarovitch and D. Corwin. 2008. Integration of Hard and Soft Data to Characterize Field-Scale Hydraulic Properties for Flow and Transport Studies *Vadose Zone J*. 7: 878-889. doi:10.2136/vzj2007.0090.

Seuntjens, P. 2002. Field-scale cadmium transport in a heterogeneous layered soil. *Water Air Soil Poll* 140: 401-423. doi:10.1023/A:1020147610743.



- Seuntjens, P., D. Mallants, N. Toride, C. Cornelis and P. Geuzens. 2001. Grid lysimeter study of steady state chloride transport in two Spodosol types using TDR and wick samplers. *J Contam Hydrol* 51: 13-39. doi:10.1016/S0169-7722(01)00120-6.
- Šimůnek, J. and J.W. Hopmans. 2002. Parameter optimization and nonlinear fitting. Method of soil analysis. Part 4. Physical methods (Dane, J.H., and Topp, G.C. Eds.). Soil Science Society of America Book Series. p. 139-157.
- Šimůnek, J., M. Šejna, H. Saito, M. Sakai and M.T. van Genuchten. 2013. The Hydrus-1D software package for simulating the movement of water, heat, and multiple solutes in variably saturated media, version 4.16, HYDRUS software series 3 Department of Environmental Sciences, University of California Riverside, Riverside, California, USA. p. 340.
- Skaggs, T.H., P.J. Shouse and J.A. Poss. 2006. Irrigating forage crops with saline waters: 2. Modeling root uptake and drainage. *Vadose Zone J* 5: 824-837. doi:10.2136/Vzj2005.0120.
- Slater, L. 2007. Near Surface Electrical Characterization of Hydraulic Conductivity: From Petrophysical Properties to Aquifer Geometries—A Review. *Surv Geophys* 28: 169-197. doi:10.1007/s10712-007-9022-y.
- Sudduth, K.A., N.R. Kitchen, W.J. Wiebold, W.D. Batchelor, G.A. Bollero, D.G. Bullock, et al. 2005. Relating apparent electrical conductivity to soil properties across the north-central USA. *Comput Electron Agr* 46: 263-283. doi:DOI 10.1016/j.compag.2004.11.010.
- Sudduth, K.A., D.B. Myers, N.R. Kitchen and S.T. Drummond. 2013. Modeling soil electrical conductivity-depth relationships with data from proximal and penetrating ECa sensors. *Geoderma* 199: 12-21. doi:DOI 10.1016/j.geoderma.2012.10.006.
- Tafteh, A. and A.R. Sepaskhah. 2012. Application of HYDRUS-1D model for simulating water and nitrate leaching from continuous and alternate furrow irrigated rapeseed and maize fields. *Agr Water Manage* 113: 19-29. doi:10.1016/j.agwat.2012.06.011.
- Taylor, S.T. and G.L. Ashcroft. 1972. Physical edaphology: The physics of irrigated and nonirrigated soils W.H. Freeman, San Francisco, CA.
- van Genuchten, M.T., F.J. Leij and S.R. Yates. 1991. The RETC code for quantifying the hydraulic functions of unsaturated soils, version 1.0. USDA, ARS, Riverside, California. .
- van Genuchten, M.T., J. Simunek, F.J. Leij, N. Toride and M. Šejna. 2012. Stanmod: Model use, calibration, and validation. *T Asabe* 55: 1353-1366.
- Verbist, K.M.J., S. Pierreux, W.M. Cornelis, R. McLaren and D. Gabriels. 2012. Parameterizing a coupled surface-subsurface three-dimensional soil hydrological model to evaluate the efficiency of a runoff water harvesting technique. *Vadose Zone J* 11. doi:10.2136/Vzj2011.0141.
- Vereecken, H., R. Kasteel, J. Vanderborght and T. Harter. 2007. Upscaling hydraulic properties and soil water flow processes in heterogeneous soils: A review. *Vadose Zone J* 6: 1-28. doi:Doi 10.2136/Vzj2006.0055.
- Vrugt, J.A., P.H. Stauffer, T. Wohling, B.A. Robinson and V.V. Vesselinov. 2008. Inverse modeling of subsurface flow and transport properties: A review with new developments. *Vadose Zone J* 7: 843-864. doi:10.2136/Vzj2007.0078.
- Vrugt, J.A., M.T. van Wijk, J.W. Hopmans and J. Simunek. 2001. One-, two-, and three-dimensional root water uptake functions for transient modeling. *Water Resour Res* 37: 2457-2470. doi:10.1029/2000wr000027.
- Walkley, A. and I.A. Black. 1934. An examination of the Degtjareff method for determining soil organic matter, and a proposed modification of the chromic acid titration method. *Soil Science* 37: 29-38.
- Wöhling, T. and J.A. Vrugt. 2011. Multiresponse multilayer vadose zone model calibration using Markov chain Monte Carlo simulation and field water retention data. *Water Resour Res* 47. doi:10.1029/2010wr009265.
- Wöhling, T., J.A. Vrugt and G.F. Barkle. 2008. Comparison of three multiobjective optimization algorithms for inverse modeling of vadose zone hydraulic properties. *Soil Sci Soc Am J* 72: 305-319. doi:10.2136/sssaj2007.0176.
- Wolf, J. 2012. LINGRA-N a grassland model for potential, water limited and N limited conditions (FORTRAN). Wageningen University, Wageningen, The Netherlands.